Fourteenth USA/Europe Air Traffic Management Research and Development Seminar (ATM2021)

Mid-air collisions with drones

Assessment of collision scenarios and of drone operation risks in urban areas

Hartmut Fricke; Stanley Förster; Robert Brühl
Chair of Air Transport Technology and Logistics
TU Dresden
Dresden, Germany
hartmut.fricke@tu-dresden.de

William J. Austen
QinetiQ Ltd
Farnborough, England
wjausten@qinetiq.com

Christoph Thiel
GfL – Gesellschaft für Luftverkehrsforschung mbH
Dresden, Germany
thiel@gfl-consult.de

Recent technological developments have led to the emergence of affordable and increasingly capable remotely-piloted aircraft or 'drones'. Aside opportunities, this also presents a potential threat to the safety of crewed aviation. This paper discusses ongoing work to evaluate and mitigate the risk and threats associated with mid-air collisions as part of initiatives to maintain and improve the high standards of aviation safety in a rapidly evolving environment. The work reported includes activities in support of two research initiatives. The first is an ongoing 'Horizon 2020'-funded project of the European Union Aviation Safety Agency (EASA) and carried out by QinetiQ in the UK, which aims to deepen the understanding of the effects of a potential mid-air collision and identify drone design strategies to mitigate their severity. The second is research at TUD that uses statistical airspeed data distributions assessed in QinetiQ's project to estimate aircraft collision risks. The risk model, which is not endorsed by EASA or QinetiQ, uses stochastically acting vehicles and pilots in an agent-based simulation, now tailored to regions where commercial drones may operate in the vicinity of airports or existing and emerging urban air operations. Work in support of QinetiQ's programme includes novel fusion and processing of large datasets (including ADS-B histories) to derive probabilistic models of potential collision speeds for different classes of aircraft; this will inform ongoing detailed collision simulation and testing studies. Work at TUD estimates probabilities for an urban scenario using that data; results indicate that management of risks within acceptable limits is possible. TUD conclude that appropriate vertical/ lateral separation to manned aviation is required for UAS operations to keep collision risks acceptable. Integration of this type of agent simulation as 'air risk' assessment in SORA is proposed.

UAS, Risk Assessment, aircraft collision speeds, vulnerability of aircraft, agent-based simulation, Target Level of Safety

Aspects of the work presented herein form part of the project 'Vulnerability of Manned Aircraft to Drone Strikes' contracted to QinetiQ Ltd by EASA and funded by the European Union's Horizon 2020 programme under grant agreement No MOVE/B3/SUB/2020-243/SI2.826742**.** This does not comprise work done at TUD.

I. INTRODUCTION

Drone products are evolving rapidly and are increasingly popular with consumers and for professional applications. There is also ongoing development of commercial platforms e.g., delivery systems, which may greatly increase the scale of drone operations and demand on airspace. Historically there have been few conflicts associated with unmanned platforms e.g., model aircraft, co-existing with crewed aircraft because their operation was traditionally on a small scale and limited to organized flying clubs and designated sites. However, modern drone products can operate from almost anywhere, exhibit high levels of performance and are operated on a much wider scale. The European Plan for Aviation Safety (EPAS) 2021-2025 [1] addresses the safety risk associated with the vulnerability of manned aircraft to drone strikes. Until the pandemic, commercial departures achieved a yearly number of up to 40 million [2, 3], and 69 million flight movements were recorded in 2019 by ADS-B transponders alone [4]. In contrast, only 24 drone collisions were identified [5] over the last 23 years, but 23 of these occurred in the last 11 years. Consequently, incident statistics show a relatively small number of reported collisions, but it is an increasing trend. Also, the number of suspected drone sighting from aircraft [6] (which may be interpreted as suspected near misses from an aviation safety perspective) are orders of magnitude greater than the number of confirmed collisions. Unless managed, these risks are likely to increase with greater unmanned urban air mobility activity in the EASA "open" (< 25 kg) and "specific" categories [7], as well as the emergence of urban air taxi vehicles in the "certified" category (> 150 kg) [8, 9]. Market studies and performance characteristics of current drones clearly identify urban and rural areas as future hot spots of drone operations. Along the European Urban Air Mobility (UAM) Initiative Cities Community (UIC^2) of the EU's Smart Cities Marketplace, new networks in the third dimension will develop over cities, aiming to best meet market expectations and business opportunities but raising societal concerns on safety, security and privacy [10].

Regulators have been working on measures to safely manage collision risks through legislation and guidance [1] and major OEMs have been developing technological solutions to mitigate risks via methods such as geo-fencing, pilot warnings, altitude

limits and more recently, ADS-B based warning systems. There are also ongoing activities to develop detection systems, counter-UAS systems and other safety related technologies. However, to maintain and improve the highest standards of aviation safety whilst also enabling the benefits of drone-based technologies and services, there is a need to understand both the potential consequences of a mid-air collision and the risk of it occurring; this will enable effective mitigations to be developed and proportionate controls to be applied.

The paper starts with a state-of-the-art review on manned aircraft threats from drones and proceeds to explore the factors that describe impact scenarios as 'collision envelope'. Common aircraft types are identified based on a large ADS-B data analysis, referring to EASA certification categories. For selected aircraft classes, a severity assessment for relevant drone impact locations is described, which aided the prioritization of more-detailed assessments by validated simulation and test in the ongoing programme. A second ADS-B big data analysis is also described, which assesses distribution of operating speeds vs. altitude. To link these trajectory profiles to probabilistic drone collision speeds, the drone sighting database [12] is used in conjunction with Monte Carlo methods. To complete the collision envelope, the selected fixed-wing and multi-rotor drones were assigned operating speeds based on a market data and reasoned use-cases. Expanding upon the collision envelope report for EASA [11], we describe how TUD injected the calculated flying characteristics into their agent-based collision risk simulation [13], focussing on altitudes below 3,000ft to evaluate an urban use case.

II. State of The Art

A. Collision threat assessments

EASA has been active in monitoring the risks and threats associated with mid-air drone collisions and the 2016 'Drone Collision Task Force' included recommendations to develop models of the drone threat and establish hazard severity thresholds for collisions between drones and manned aircraft [14]. To progress this work, EASA tendered a scoping study, including work packages to refine the definition of the UAS threat, undertake a Bow-Tie based risk assessment and define an outline programme of research that would enable the severity of a broad range of collision scenarios between multiple types of aircraft and drone to be evaluated [15, 16]. EASA subsequently tendered an updated programme and awarded it to QinetiQ in the UK. This programme aims to deepen understanding of the effects of potential mid-air collisions, identify drone design strategies to reduce the severity of outcome and draft drone design/test requirements to mitigate the collision threat. The initial research and planning stages (Tasks 1 to 3) are now complete and collision assessment activities are underway, including development of finite element-based models and full-scale impact testing against aircraft structures. Task 1 included review of the worldwide state-of-the-art in drone collision modelling [5], which contains a summary and outcome of other major activities such as the FAA-sponsored ASSURE initiative and QinetiQ's work on windshield impacts. Task 2 established a 'Collision Envelope', which is discussed further in Section III, and Task 3 consolidated findings into plans for the modelling and experimental phase.

B. Collision risk assessments

Standard approaches for the safety risk assessment of UAS operations as in [17, 18] consist of the identification of potential hazards, the assessment with regard to severity and probability of occurrence and the mitigation of hazards exceeding a given acceptance level. To further develop sense and avoid systems of UAS, a risk-based separation model is introduced by Weibel et al. [19] relying on their 3D contours. In the encounter model, risk probability is calculated as the proportion of trajectories in the near mid-air collision (NMAC) cylinders on all trajectories in a certain state around the UAS. EASA's Task Force [14] established a risk assessment model by identifying the key critical components of the UAS and the critical structures of manned aircraft and determining the effects between them after a collision. Severities were associated per aircraft component and the risk qualitatively assessed. McFadyen and Martin [20] calculated the vertical overlap probability of manned aircraft and UAS based on departure/ arrival trajectories. For the altitude distribution function of manned aircraft, position data were used. In case of the UAS, analytical models were considered. The behaviour of the UAS and the manned aircraft led to distribution functions of the vertical separation and overlap probability. McFadyen, Martin and Perez [21] estimated the total collision risk including 3D and spatial-temporal overlap probability by modelling the airspace as a grid in all dimensions and the flight paths as located data points. For the 3D overlap probability in every cell, the position data of the aircraft and the simulation data of the UAS were considered. To estimate the temporary overlap probability, multiple scenarios over cell agglomerations were studied. Zhang et al. [22] presented an approach for the NMAC fatality risk estimation based on the gas model of aircraft collisions. The risk is finally assessed by modelling the estimation of the frequency of fatalities and using simulations for the evaluation. This frequency takes into consideration the relative collision areas and speeds of both the UAS and aircraft.

III. Establishing a Collision Envelope

The evaluation of collision risks and outcomes requires impact scenarios to be defined. The key variables associated with these scenarios are described as the 'collision envelope' and include the type of drone, type of aircraft, their relative velocities, and the impact location. The collision envelope developed for EASA is reported in [11] and is summarized herein, with particular focus on the processing of historical air traffic data to inform the identification of popular aircraft types and evaluate credible collision speeds. When evaluating collision risks in an urban environment via agent-based simulations [13, 23] it was also necessary to establish navigation tolerances; these were based upon empirical data for crewed aircraft and – due to a lack of historic data - scenario-based for drones.

A. Aircraft type selection and classification

The scope of the vulnerability programme includes aircraft within the following EASA Certification Specifications (CS, see also Table 1): CS-23, CS-25, CS27, and CS-29 [24]. Example aircraft were identified for each of these classes, based on

statistical usage data. ADS-B traffic and surveillance data was taken from Open Sky Network [6], encompassing the entire German airspace at altitudes up to FL 120 for the full year 2019, leading to roughly 1.7 x 10^9 data points. This data was sampled to 30 random days, filtered for outliers and anomalies. The FL 120 altitude boundary is considered to conservatively cover typical consumer/ prosumer drone operations and is based on statistical evidence (see section IV.B). This vertical band was reduced to FL30 in follow-on activities, exploring urban area safety considerations.

Since the reference data set does not contain information on the aircraft model itself, the ICAO 24-bit (Mode S) identifier of the on-board transponder was used to assign the corresponding airframe (including manufacturer, model, type-code and ICAO-type). Required link information was taken from the OSN airframe database [6]. In particular, the model and the ICAO-type were used to filter and group results by aircraft type (Land Plane (L), Helicopter(H)) and count/ type of engines (Jet (J), Piston (P), Turboprop/Turboshaft (T)), broken further down into relevant candidates per CS category.

Figure 1. depicts the statistical/ expert driven determination process of the representative aircraft type for the exemplar CS-23 category (although not required to have ADS-B capable Mode S transponder installed):

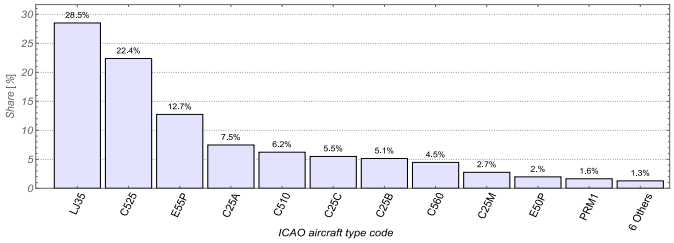

Figure 1. Identified types in ADS-B data set, CS-23 Jets category

In addition to the CS-23, CS-25, CS-27 and CS-29 classes, consideration was also given to future VTOL configurations such as the Volocopter Volocity [8] and the Lillium Jet [9]. However, these are not formally within the scope of the current EASA vulnerability programme. This way, the following example aircraft types were derived:

- CS-23 Single Prop: Cessna 172 SkyHawk,
- CS-23 Jets: Cessna 510 Citation Mustang,
- CS-25: Airbus A320,
- CS-27: Robinson R44,
- CS-29: Airbus H-145,
- Future Aircraft SC-VTOL: Volocity/ Lillium as sole candidates, no statistical evidence.

It was recognized that the above classes encompass a wide variety of aircraft configurations, sizes, and performance capabilities. We therefore sub-divided them further, using parameters available from the ICAO identifier, when evaluating statistical flight speeds (see section IV). Eight aircraft sub-classes (AC) were established from the four primary EASA categories, as shown in Table 1:

Class	Description
AC1	Large Jet Aircraft with MTOM > 8618 kg (CS-25)
AC2	Large Turboprops with MTOM > 8618 kg (CS-25)
AC3	Small Jet Aircraft with MTOM ≤ 8618 kg (CS-23)
AC4	Small Turboprops with MTOM ≤ 8618 kg (CS-23)
AC5	Piston aircraft with 2 engines (CS-23)
AC6	Piston aircraft with 1 engine (CS-23)
AC7	Large Helicopters with MTOM > 3175 kg (CS-29)
AC8	Small Helicopters with MTOM ≤ 3175 kg (CS-27)

Table 1: Identified aircraft classes for collision speed clustering

B. *Local manned aircraft target identification*

The vulnerability programme will involve detailed finite element analysis and testing of collision scenarios, but it would not be practical to consider impacts against all potential impact sites on each aircraft class: We instead prioritized the local impact zones of interest. A detailed description of this process is beyond the scope of this paper, but a summary is provided, and further information can be found in [11].

A list of candidate impact zones e.g., windshields/ propellers/ leading edges, was created based upon outputs from EASA's Drone Collision Task Force report [25], findings from other studies [5] and input from subject matter experts. For each example aircraft, these zones were evaluated against the criteria *relative probability* of a feature being impacted, *perceived vulnerability* of the feature to impact damage, and the *criticality* of the feature to the safety of the aircraft and its crew & passengers. This was achieved via a combination of workshops and off-line surveys involving industry professionals, regulators and representatives of major aircraft and drone OEMs.

1) *Conditional probability*

The conditional probabilities assume that a collision has occurred and considered the relative probability of each of the candidate impact zones will be struck. The assessment generally assumed that the aircraft is in forward flight, though it was acknowledged that rotorcraft could be struck whilst in hover or low-speed manoeuvres.

Inarguably small features such as pitot static assemblies were assigned a 'low' probability classification and it was also agreed that the same should apply to control surfaces (excluding high-lift devices). The remaining impact zones were assessed by calculating their individual projected frontal areas as a proportion of the frontal area of the airframe. This was achieved by constructing silhouettes. Figure 2. shows an example construction for the CS-29 category:

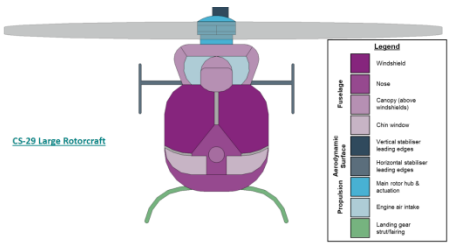

Figure 2. Rotorcraft silhouettes for frontal area calculation, CS-29 category

Each silhouette was partitioned to represent the applicable impact zones and the relative areas calculated. Impact zones with an area less than 5% were classified 'low' probability,

zones with >20% 'high'. Propellers and rotors were assigned 'high' probability ratings based upon their large swept area.

2) Vulnerability

This classification addresses the perceived robustness of the impact zones and their ability to withstand an impact without failure. The three-level determination was based upon expert opinion and evidence [5].

3) Criticality

The perceived safety impact of the impact zone being damaged was classified on a four-point scale, from 'low' to 'extreme' (immediate, grave threat).

Finally, a manual process to prioritize the impact zones based upon the combined assessment of these criteria was executed, leading to the following list:

Impact location		Priority classification				
		CS-25 Large Aeroplane	**CS-23 Jet**	**CS-23 Single Prop**	**CS-27 Small Rotorcraft**	**CS-29 Large Rotorcraft**
Fuselage	Radome	Medium	Medium	Medium	Medium	Medium
	Nose	High	Medium	High	High	Medium
	Canopy (above windshields)	High	N/A	N/A	Medium	Medium
	Windshield	High	High	High	High	High
	Chain window (rotorcraft)	N/A	N/A	N/A	High	High
	Side window	N/A	N/A	N/A	Low	Low
	Fuselage sides/rear	N/A	N/A	N/A	Low	Low
Aerodynamic surfaces	Wing leading edge	Medium	High	High	N/A	N/A
	Wing braces	N/A	N/A	High	N/A	N/A
	Wing slats	Medium	N/A	N/A	N/A	N/A
	Wing flaps	Medium	Medium	Medium	N/A	N/A
	Winglet leading edge	Medium	N/A	N/A	N/A	N/A
	Wing root fairings	Low	Low	Low	N/A	N/A
	Vertical stabilizer leading edges	High	High	High	Medium	Medium
	Horizontal stabilizer leading edges	High	High	High	Medium	Medium
	Rudder/Ailerons, spoilers or elevators	Medium	Medium	Medium	N/A	N/A
Fixed wing propulsion	Engines (excluding reciprocating engines)	High	High	N/A	N/A	N/A
	Engine (reciprocating)	N/A	N/A	Medium	N/A	N/A
	Propellers	Medium	N/A	High	N/A	N/A
	Engine pylons	Low	Low	N/A	N/A	N/A
	Engine nacelle leading edges	Medium	Medium	N/A	N/A	N/A
Rotorcraft propulsion	Main rotor	N/A	N/A	N/A	High	High
	Tail rotor	N/A	N/A	N/A	High	High
	Main rotor hub & actuation	N/A	N/A	N/A	High	High
	Tail rotor hub & actuation	N/A	N/A	N/A	High	High
	Main rotor hub fairing/ Mast	N/A	N/A	N/A	Medium	Low
	Engine air intake	N/A	N/A	N/A	Low	Low
Gear	Wheels	Low	Medium	Medium	N/A	N/A
	Landing gear strut/fairing	Medium	Medium	Medium	Medium	Low
	Undercarriage housing/ Fairing	N/A	N/A	Medium	N/A	Low
	Gear bay doors	Medium	Low	Low	Low	N/A
Systems	Lights	Low	Low	Low	Low	Low
	Pilot tubes	Low	Low	Low	Low	Low
	External antennas	Low	Low	Low	Low	Low
	Auxiliary Power Unit & Environmental Control Systems intake	Low	N/A	N/A	N/A	N/A
P r	*Priority Ranking based upon the assessment of **probability** of a region being stuck **critically** of the area to save flight and perceived **vulnerability** to damage*	Low	Low priority – Qualitative assessment suggests that risk to safety is relatively low			
		Medium	Medium priority – Judged to be a credible risk to safety and beneficial to assess but not a priority			
		High	High priority – Project should investigate how to assess threat			
		N/A	No relevant to the aircraft configuration			

Table 2 Prioritized aircraft impact zones, all categories

This matrix served to identify the features on each class of aircraft that should be assessed in greater detail. Activities are currently underway to evaluate the 'High' priority items by analysis and/ or test as part of the ongoing vulnerability programme or through collaboration with other programmes.

In section IV, we investigate the speeds of all aircraft classes, serving as crucial inputs to the collision modelling. They also inform the TUD collision probability estimation activities outside the vulnerability programme in sections V and VI.

IV. Aircraft & Drone Collision Speeds

The approach taken by other drone collision studies to-date has been to assume nominal or upper-bound aircraft speeds associated with relevant phases of flight e.g., climb-out, or final approach. However, these are not constant, and a spectrum of speeds would be expected during normal operation. This section evaluates the probabilistic distribution of aircraft speeds at different operating altitudes (with particular focus on heights at which drones are likely to operate) and statistically mean collision speeds based upon historical mid-air drone sightings.

A. Manned Aircraft Speeds over Altitude

Aircraft operating speed is typically given as indicated, body fixed air speed (IAS) to account for the aerodynamic properties of the vehicle. Those depend on atmospheric parameters, altering with altitude. IAS has to convert to true and then to ground speeds for energy modelling. True air speed (TAS) conversion - to consider compressibility and temperature corrections - is given by:

$$TAS = IAS\frac{171{,}233\sqrt{288 + (T - T_{ISA}) - 0.006496 \cdot h}}{(288 - 0.006496 \cdot h)^{2.628}}$$

with T-T_{ISA} = Temperature relative to ISA in °C, h = altitude in m [26]. Ground Speed (GS) is given by GS = TAS + Wind Component.

To determine the individual speeds of manned aircraft, we also use statistical flight data taken from ADS-B repositories [6] as a function of altitude. ADS-B data is composed of standard information items as shown in Table 3.

timestamp	2019-05-31 00:00:01		
altitude	2392.68	1127.76	274.32
callsign	PGT5CD	BCS192	PGT4Y
geo-altitude	2567.94	NaN	381.00
groundspeed	138.346226	114.248272	64.089069
icao24	4b906d	407494	4b8490
latitude	52.338135	50.741287	50.820053
longitude	10.417480	7.460709	7.216681
squawk	1000.0	4153.0	1172.0
track	292.750976	231.581945	317.602562
vertical rate	-4.87680	-7.47776	-3.90144

Table 3 ADS-B standard data structure [6]

Meteorological data from Deutsche Wetterdienst (DWD) [27, 28] was used to provide temperature, wind direction, wind speed, and static air pressure across a large (>100) set of meteorological stations. These local measurements were used to compute the wind at any ADS-B data point, based on an interpolation as a weighted arithmetic mean of the three closest stations at 10 min temporal resolution. To convert from geo(metric) altitude above MSL (2nd line in Table 3) to geodetic altitude, the digital terrain model "DGM200" was used. The horizontal resolution is 200m, the vertical 1cm, the accuracy +/- 5m and +/- 3m respectively [29]. Day, evening, and night distinction was also taken into consideration to distinguish operations following SERA definition [30]. A grid with civil dusk/ dawn times at individual geographical positions for every single day of the year 2019 was introduced.

Individual speeds per aircraft sub-class were required (section III.A), so it was necessary to utilise available metrics e.g., type/ propulsion system and maximum take-off mass (MTOM) to filter the data. For all aircraft models, MTOM was extracted from the EUROCONTROL Aircraft Performance Database [31] (~70 % of aircraft), else taken from the EUROCONTROL SKYbrary repository [32] (~20 %), else from official manufacturer, supplier handbooks or specification sheets (~10 %).

From the ADS-B data acquired, 30 representative days were randomly selected. The processed data was statistically analyzed for mean, standard deviation and specific quantiles per aircraft class and altitude band (below 5,000 ft GND, 500 ft resolution, else a 1,000 ft increment). The following figure depicts the results for a selected aircraft class (AC). Further, information on the following statistical parameters was gathered including share of aircraft types and so MTOM distribution within the given AC, and ground speed distribution per altitude band. Based on statistical evidence, it was concluded that the data fitted a normal distribution for all aircraft classes (see lower picture series in Figure 3.).

The statistical analysis of this 'baseline' scenario showed expectable behaviour for all AC, ground speed, altitude, and aircraft size. Operating speeds are sensitive to prevailing wind conditions and daytime due to aerodynamic and safety reasons. Consequently, the sample data was further analyzed

- with a wind speed threshold active to form a 'low wind scenario' (<= 2 m/s mean wind speed the last 10 min),
- with both a wind speed threshold and a night indicator active to form a 'safe drone operations scenario' (<=10 m/s mean wind speed, no night-time operations).

The output in tabular format for e.g., CS29 large rotorcraft (AC7, see Table 1) reads according to Table 4:

Altitude Band [ft]	N	Mean	SD	$Q_{0.05}$	$Q_{0.5}$	$Q_{0.95}$	$Q_{0.99}$
50 - 500	256,435	36	30	2,24	28,43	102,47	123,43
500 - 1000	548,456	89	36	12,37	100,24	133,7	144,51
1000 - 1500	596,833	102	36	12,04	112,68	140,89	153,23
1500 - 2000	371,966	103	39	9,22	116,3	144,63	156,19
2,000 – 2,500	186,408	112	34	18,87	121,02	153,26	162,73
2,500 – 3,000	84,441	117	26	66,6	123,43	148,07	156,78

- Table 4 Ground speed distribution over height– CS 29 helicopters (AC7)

The same excerpt in graphic format reads for AC5:

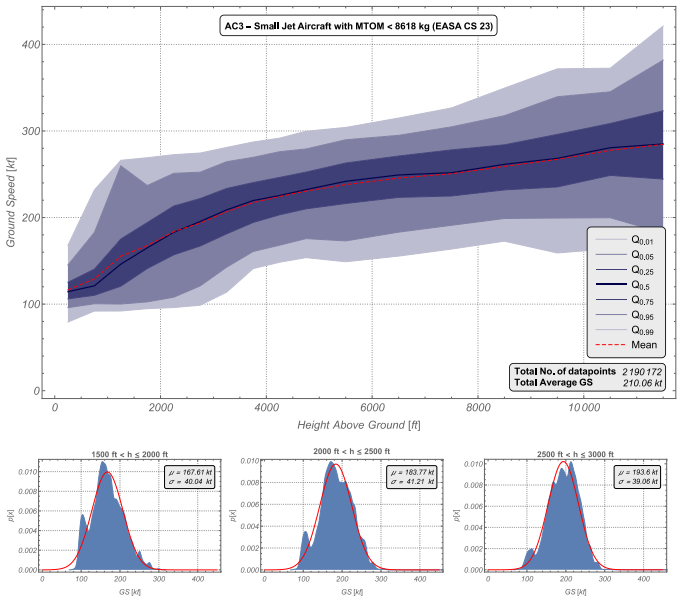

Figure 3. Ground speed distribution over height– CS23 small jets (AC5)

Comparing both wind scenarios leads to:

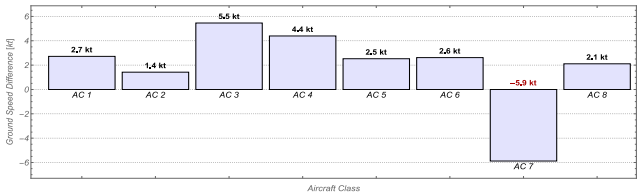

Figure 4. Mean Ground speed changes 'low-wind' vs. 'baseline' scenario

For fixed-wing aircraft the outcome in the low wind scenario shows a higher average ground speed because low altitude operations (approach and departures) are usually run with headwind. The singular decrease found for the helicopter class (AC7) however can only be explained with statistical effects of very few data points. Similar effects were found when comparing to the safe drone operations according to Figure 5.

It was concluded that these external factors have a minor (and generally positive) effect on the data, while some statistical confidence is lost due to reduced data. So, the baseline is used.

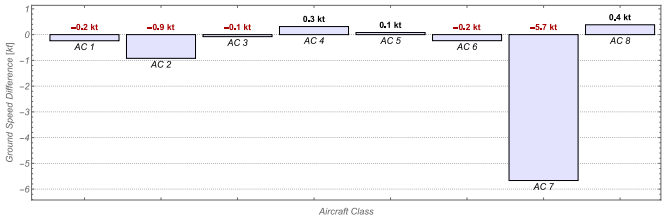

Figure 5. Mean Ground speed changes 'safe drone ops' vs. 'baseline'

B. *Drone altitude - sightings*

We described how the probabilistic distribution of aircraft ground speeds was calculated as a function of altitude. This provides an evidence-based justification for the speed of different categories of aircraft during lower-altitude phases of

flight, rather than relying upon generalized performance figures. When considering near mid-air collisions (NMAC) with drones, the relative velocity of the drone to the aircraft is the second most relevant risk trigger. If a similar database of drone movements were available, then a detailed analysis of potential encounters could be undertaken. However, such a database is not known to exist.

Altitude and speed drone capabilities rely on their performance specifications, but this does not indicate as to how they are used in practice. Instead, an alternative approach was developed, based on a database of drone sightings (or 'near misses') collated by the Aviation Safety Network [12]. This database contains over 12,000 entries documenting world-wide drone sightings from aircraft and un-/ confirmed collisions. It has constantly been compiled from a wide range of referenced sources. A query of sighting altitude over frequency produces the logarithmic-type correlation as depicted in Figure 6. It shows, that roughly 50% of all sightings were found below 3,000 ft and as such well in the level band of intermediate/ final approaches and initial climb out of manned aircraft: Most entries in this database are based upon reported in-flight drone sightings and so the individual data veracity cannot be fully verified. Despite these limitations, it represents a large, relevant dataset which is assumed to be appropriate for the purpose of defining an approximate distribution of drones by altitude.

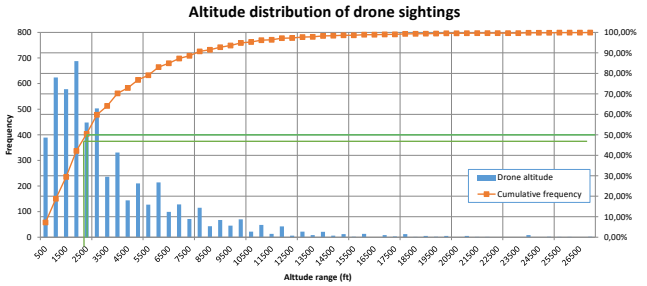

Figure 6. Drone sightings by altitude, generated based on [12]

To emphasize on the growing relevance of drone collision risk, the same database allows to sort chronologically sightings, especially those judged as 'near-misses' according to Figure 7.

A statistical quality indicator to judge the severity of these near misses was developed using the estimated vertical separation to the drone at closest approach point, based on [27].

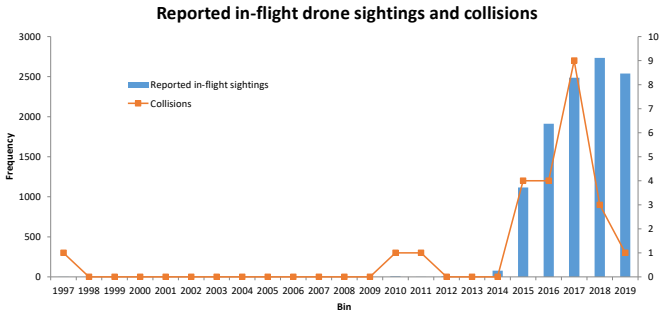

Figure 7. Reported in-flight drone sightings & collisions, based on [12]

C. *Fixed wing drone speeds*

The performance capabilities of drone products are given in their specifications thus representing limiting, rather than typical values.

Drones can accelerate rapidly and are not bound by the same procedural limits as manned aircraft during approach and departure. Therefore, the speeds of fixed wing and multi-rotor drones are not linked to altitude in the same way. I.e., the speed of a drone is rather depending on the operator's intent. Fixed wing drones operate within a velocity range between stall and maximum flight speed (equivalent to v_{NE} for classic aircraft). In low-level scenarios (e.g., below 500 ft), where the drone is doing circuits within line of sight, the actual speed may vary considerably between these limits, depending upon the skill and aggressiveness of the operator. The greatest speeds are achieved with combinations of thrust and manoeuvers, so upper-bound speeds are highly transient and not sustained. A maximum low-level velocity of 23 m/s was derived for generic configurations, based upon the quoted performance of fixed wing drones such as the Parrot Disco, Yuneec Firebird, and the former Parcelcopter 4.0. If intending to fly at higher altitudes for larger distances, operators are likely to fly at the drone's cruise speed to maximise range. We assume a cruise speed of 23 m/s, which is compatible with assumptions made in EASA's counter-unmanned air system activities [33].

The above speeds are intended to provide guidance for generic fixed wing drone configurations. As for the use case in this study, we refer specifically to the Parcelcopter-like vehicle speed of 36 m/s and configuration (see section VI).

D. *Multi-rotor drone speeds*

Multi-rotor flight can be flown very differently: In low level scenarios, speeds will depend upon type of drone and operator's skill. These may credibly range from hovering manoeuvres to full-speed runs under manual control ('stabilized' modes for most drone types but Racing-Style configurations may also have 'Acro' mode for greater speed and manoeuvrability). A realistic height limit for fast, aggressive manual flying is assumed to be 500 ft. In mid-level scenarios (between 500 ft and 1,000 ft), endurance or range maximization is assumed, so using max range speed. For high-level flight (greater than 1,000 ft), it is assumed that altitude is the objective. So, drone would have minimal ground speed to avoid drifting away from the operator.

	DJI Mavic Mini	**DJI Mavic 2**	**Low cost, Racing style**	**DJI Inspire 2**
Maximum speed (Sport mode on)	13 m/s	20 m/s	~27 m/s	26.1 m/s
	25.3 kts	38.9 kts	52.5 kts	50.8 kts
Cruise speed (Sport mode off)	8 m/s	13.9 m/s	~15 m/s	8 m/s
	15.6 kts	27 kts	29 kts	15.6 kts

Table 5 Multi-rotor flight speeds according to market survey

E. *Collision orientation*

Comprehensive definition of a collision between two vehicles in free space involves many variables, though these may be of differing levels of importance to the outcome of the event. Primary variables include the location that the drone strikes the aircraft and their relative speeds. Secondary variables describe the relative angles of yaw, pitch and roll of the vehicles,

and tertiary variables include sideslip and rise/sink rates as well as rotational velocities at the time of impact.

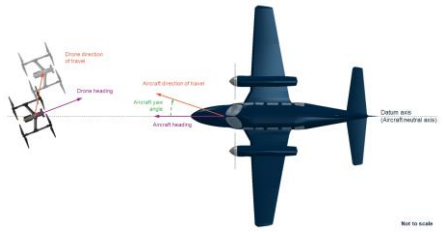

Figure 8. Excerpt: Illustration of discussed yaw conditions

For the sake of first order insights into collision risk of drones threatening commercial aircraft however, we limit the scope to the primary variables and keep all other as presumably worst case, i.e., assuming head-on impacts with nominal pitch and yaw conditions. This may be revisited once detailed drone models can be used to explore the relative severity of different impact orientations.

F. Aircraft collision speeds

Monte Carlo analysis was used to combine the manned aircraft flight data per altitude results with the drone sighting and collision data. This assumed that the distribution of mid-flight drone sightings is representative of 'near misses' which could equally have been collisions in less fortunate circumstances.

The results of the aircraft flight survey included clustered mean speeds and standard deviations (see Figure 3. Table 2) and baseline scenario conditions.

The analysis refers to the altitude of each of the unambiguous 5,255 'near misses' out of the +12,000 ASN entries: The near-miss altitude was matched with the relevant flight survey altitude band and the corresponding speed characteristics identified. A speed was then calculated using a random sampling of the Gaussian distribution. This process was repeated 100 times for each near-miss altitude and for all classes. After normalization, Figure 9. depicts the aircraft speed per AC at assumed collision altitude as probability densities.

The quantiles result to the numerical values as shown in Table 6:

Percentile speed [kts] per AC	50th	75th	95th	99th
AC1	189	245	312	354
AC2	184	225	274	305
AC3	196	236	289	330
AC4	165	195	245	285
AC5	137	156	183	202
AC6	112	139	180	207
AC7	127	143	168	191
AC8	105	127	159	184

Table 6 Percentile aircraft speeds [kts] in NMAC drone collisions, baseline

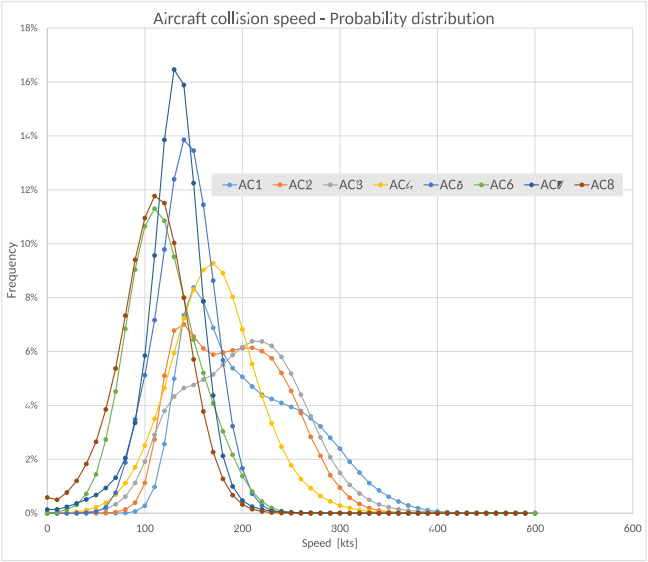

Figure 9. Probability density distributions of manned aircraft collision speeds for historical drone sightings, all AC

V. AGENT BASED COLLISION RISK MODELLING

For many years of research in the field of safety in aviation TUD developed an agent-based terminal airspace simulation within various research projects, outside EASA's vulnerability programme [13, 23]. It comprises aircraft, pilot, and ATC models being simulated with a focus on the interactions of human and technical system per entity (e.g., the aircraft). It assesses aircraft collision risk for modern instrument flight procedures, focusing on the intermediate and final approach. The aircraft's, ATCO and CNS systems' behaviours are modelled as stochastically acting agents using a Monte-Carlo simulation engine to represent a statistically realistic environment [13]. We integrated the assessed airspeed distributions (see Chapter IV) as additional parameter set into the simulation tool to build a fast-time collision risk model addressing crossing drone operations in the terminal area of an airport with single runway operations. This mid-size character seems appropriate to typical drone use cases. Aside other, aircraft and drone behave as agents with epistemic behaviour concerning cross, along, and vertical navigation tolerances (XTT, ATT, VTT) and aircraft speed based on the findings in section IV.

The navigation tolerances are modelled as a function of the distance to go (threshold distance) [34, 35]. Since no historic drone specific tolerance data yet exist, we apply a scenario technique assuming a) a 10-fold increase in tolerances compared to manned aircraft due to much less standardized remote pilot behaviour and – more optimistic - b) only a 5fold increase. Assuming visual guidance, the navigation tolerances for drones are modelled as linearly dependent on distance from vertiport, which leads to diamond-like tolerance characteristics, as known from classic aeronautical navigation like VOR/DME. As part of the risk sensitivity analyses, we place the drone leg westerly with offsets from 0 m to 200 m to the 04 DRS final approach.

Within the simulation environment, route networks are modelled as directed acyclic graphs (DAC) where nodes

represent waypoints or air-/ vertiport locations. For each network, a traffic source is configured accordingly to generate aircraft and drone entities, respectively. For each type of entity, a speed distribution and its navigation tolerances can be set independently. Traffic load is adjusted either by setting a traffic frequency or providing a distribution over in-trail separation. No ATCO agents are instantiated for the presented study.

VI. Dresden – An Urban Area Use Case

A. Use case configuration

In this section, we study the outcome of the tailored agent-based simulation (see section V), to assess model plausibility with risk estimates for the chosen model parameters and scenarios.

The hypothesis is that instead of implementing no fly zones (NFZ) around these crucial infrastructures according to [7], tailored traffic constraints and leg geometries may present suitable risk mitigation measures to keep current levels of safety in aviation while widening the door to new drone related business cases. Once specific nav data for drone operations become available, validation experiments will follow. The built use case implies some simplifications to keep complexity reasonable and allow drawing transparent cause-effect conclusions. These include the findings in section IV such as collisions are treated as head-on conflicts, vertical occurrence probability follows sighting distribution (Figure 6.), and severity classes allocated conservatively to 'catastrophic`. As for the traffic demand, we will assess a **nominal** and a **peak load** (worst case) scenario. We choose greater Dresden area, Saxony, Germany for which the following simplifications were made:

- Implementation of one, a Parcelcopter-like drone type (operating air speed of up to 36 m/s, see section IV.C)
- One single DHL drone network link with varying distance from DRS 04 approach, from 16 km connecting a small drone depot outside Dresden with the parcel downtown centre crossing the final approach at a small angle of 2.8° (red line = baseline, blue line = offset drone leg in Figure 10.)
- The simulation of manned aircraft established on DRS 04 final (black line in Figure 10), uniformly represented by CS-25 example aircraft.

We assume aircraft frequencies on DRS final approach track 04/22 derived from typical demand at small/medium sized airports with a single runway: Based on a nominal 3 NM separation [36], (90 s minimum interarrival time), this leads to a technical capacity of 40 landings/peak hour scenario in single mode. Further we study 12 landings/ normal hour scenario, based on typical traffic demand for the given airport size. For the drone transport demand model, we assume 12 million daily parcel deliveries in Germany [37]. The group of Deutsche Post DHL (DPDHL) had the largest share of this volume with 57% [38] which will be considered as representative for Dresden.

The parcel demand was built upon the following assumptions:

- delivery rate in Germany = 24 parcels/ year and inhabitant [39]. Dresden inhabitants: 555,000 [40].
- time critical, drone favoured parcels equal 4% [41].
- only parcels up to 2.3 kg to be transported with a drone [42], corresponding to app. 90% of all parcels [43]. Total payload of the drone is 4 kg, leading to single/ combined parcel packages (1 to 4 kg/parcel).
- resulting in up to 56 drone ops/ peak hour and 36 flights/ normal hour.

Figure 10. Use case Scenario, drone leg (red, baseline/blue, offset scenarios), linking two drone parcel stations, crossing DRS final approach track (black)

B. Collision risks

Based on the above setting, we simulated a total of 28 different scenarios. Wind fields were not considered, aircraft ground speed equals TAS as depicted in section IV.F, depending on altitude. Drone speeds are modelled as normal distribution with μ=25 m/s and σ=2.8 m/s to account for relatively high fluctuation resulting from atmospheric sensitivity due to low inertia, and manual guidance effects. The ANP factor of drones compared to aircraft is set to 5 resp. 10, see section V. The route network for DRS airport is taken from AIP charts, while only traffic along final approach is simulated. The drone leg requires a fixed drone operating altitude, varied between 1,000 and 1,800 feet at 200 feet steps (airport elevation is 755 ft). Each scenario comprises a total of one million simulated hours. For each aircraft-drone pair that appears to coexist within the simulation, a collision risk is associated, which is then summed up over the scenario, finally divided by the total number of flight hours in approach to derive a collision probability per flight hour. The results of the simulations are presented in Figure 11. From the results, TUD derive four key findings, for which we clearly state, that they are not implicitly or explicitly endorsed by EASA or QinetiQ:

1. For configurations where drone and aircraft tracks intersect, we observe the so-called navigation paradox, which states that smaller ANP lead to higher collision probabilities. This is a result of higher spatial concentration of traffic along the route and thus less dispersion of traffic especially at the point where final approach and drone leg intersect. This effect is a result from missing temporal dependency of both traffic streams as set in the simulation. We see confirmation of this effect disappearing at altitudes such that the drone leg surpasses the final approach leg.

2. The traffic load's effect on collision probability is less significant than expected. Hence, capping capacity via a reduced frequency of drone traffic in favour of NFZ as risk mitigation may not be as effective as expected.
3. The most sensitive variables that influence collision risk are lateral and vertical separation of drone and aircraft tracks, respectively.
4. Without any risk mitigation in place, the overall collision probability is relatively high and confirms the relevance of smart drone airspace integration strategies. However, we are aware that only exceptional collisions will be of fatal severity, the majority rather of limited impact, depending upon the impact parameters. Comparing safety target levels with manned aviation this would lead to a downgrade by two orders of magnitude per severity category according to ICAO risk matrix [36], which requires next steps to model more detailed use cases including geometric considerations (see section IV.E).

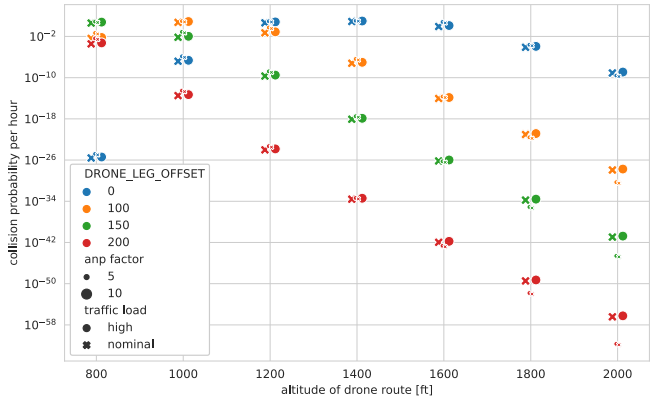

Figure 11. Collision probability per hour in approach and altitude, agent simulation results for all scenarios. (Note: Markers are jittered along x-axis around categorical altitude values to improve visual distinction.)

VII. Conclusions

In support of QinetiQ's vulnerability study for EASA, a significant 'big data' exercise has been performed, including the fusion of multiple unrelated datasets, to provide a probabilistic assessment of potential collision speeds. This, coupled with work to identify common aircraft types and exercises to define a 'collision envelope' provides a robust foundation for the ongoing activities to evaluate collision scenarios by validated modelling and test in a major European research programme.

In a separate activity, TUD used that data to assess aircraft – drone collision risks based on their mature, in-house agent simulation toolsets. TUD concluded that facilitation of drone business can be reached by designing airspace structures based on such operations risk assessments. As emerging commercial drone use cases are considered likely to fit within the specific category [7], TUD suggest integrating this type of agent simulation as air risk assessment in SORA [7]. This way, new market opportunities may materialize while coping with existing safety levels accepted for manned aviation by ICAO. As next step, TUD will perform measurements on nominal ANP to narrow down uncertainty of the presented use case and open the floor for validation.

References

[1] European Aviation Safety Agency, *The European Plan for Aviation Safety (EPAS 2021-2025).* [Online]. Available: https://www.easa.europa.eu/sites/default/files/dfu/epas_2021_2025_vol_one_final.pdf (accessed: Mar. 22 2021).

[2] International Civil Aviation Organisation, *The World of Air Transport in 2018.* [Online]. Available: https://www.icao.int/annual-report-2018/Pages/the-world-of-air-transport-in-2018.aspx (accessed: Mar. 22 2021).

[3] E. Mazareanu, *Airline industry worldwide - number of flights 2004-2021.* [Online]. Available: https://www.statista.com/statistics/564769/airline-industry-number-of-flights/ (accessed: Mar. 22 2021).

[4] I. Petchenik, *Year 2019 - by the numbers.* [Online]. Available: https://www.flightradar24.com/blog/flightradar24s-2019-by-the-numbers/ (accessed: Mar. 22 2021).

[5] W. J. Austen, S. J. Lord, and S. A. Bridges, *Analysis of the state-of-the-art (D1.3), and Research Cooperation (D1.4).* [Online]. Available: https://www.easa.europa.eu/sites/default/files/dfu/deliverable-analysis_of_the_state-of-the-art_d1.3_and_research_cooperation_d1.4.pdf (accessed: Apr. 10 2021).

[6] S. Schäfer, M. Strohmeier, V. Lenders, I. Martinovic, and M. Wilhelm, "Bringing up OpenSky: A large-scale ADS-B sensor network for research," in *IPSN-14 Proceedings of the 13th International Symposium on Information Processing in Sensor Networks*, Berlin, Germany, 2014, pp. 83–94.

[7] EU Commission, *Durchführungsverordnung (EU) 2019/ 947 DER KOMMISSION - vom 24. Mai 2019 - über die Vorschriften und Verfahren für den Betrieb unbemannter Luftfahrzeuge*, 2019. Accessed: Mar. 22 2021. [Online]. Available: https://eur-lex.europa.eu/legal-content/DE/TXT/PDF/?uri=CELEX:32019R0947

[8] Volocopter GmbH, *Volocopter - VoloCity.* [Online]. Available: https://www.volocopter.com/en/product/ (accessed: Mar. 20 2021).

[9] Lilium GmbH, *Introducing the Lilium Jet.* [Online]. Available: https://lilium.com/the-jet (accessed: Mar. 20 2021).

[10] Federal Ministry of Transport and Digital Infrastructure, *Operation of drones in German airspace: transport policy challenges and the conflicting demands of innovation, safety, security and privacy.* [Online]. Available: https://tu-dresden.de/bu/verkehr/ila/ifl/ressourcen/dateien/kooperation/beirat/2019/Final-Engl-_Umgang_Drohnen_2-3_hf.pdf?lang=de (accessed: Feb. 12 2021).

[11] EASA European Aviation Safety Agency, *Collision envelope specification and justification report (D2.1): Vulnerability of Manned Aircraft to Drone Strikes.* [Online]. Available: https://www.easa.europa.eu/research-projects/vulnerability-manned-aircraft-drone-strikes (accessed: Apr. 5 2021).

[12] ASN Aviation Safety Network, *ASN Drone Database.* [Online]. Available: https://aviation-safety.net/database/issue/dronedb.php (accessed: Apr. 11 2021).

[13] H. Fricke, S. Forster, and M. Vogel, "Using agent-based modeling to determine collision risk in complex TMA environments: the turn-onto-ILS-final safety case," *AAOAJ*, vol. 2, no. 3, 2018, doi: 10.15406/aaoaj.2018.02.00046.

[14] European Aviation Safety Agency, *'Drone Collision' Task Force: Final Report.* [Online]. Available: https://www.easa.europa.eu/document-library/general-publications/drone-collision-task-force (accessed: Apr. 11 2021).

[15] W. J. Austen and S. J. Lord, *Report on Research Programme on Collisions with Drones: Work Area 1 - Final Report.* [Online]. Available: https://www.easa.europa.eu/sites/default/files/dfu/QinetiQ%20-%20EASA.2016.LVP_.50%20UAS%20Collisions%20-%20Report%20WA1-%20Issue%204.0%20-%20For%20publication%20-%20NS.pdf (accessed: Feb. 12 2021).

[16] W. J. Austen, *Report on Research Programme on Collisions with Drones: Work Areas 2-5 - Final Report.* [Online]. Available: https://www.easa.europa.eu/sites/default/files/dfu/QinetiQ%20-%20EASA.2016.LVP_.50%20UAS%20Collisions%20-%20Report%20WA2-5%20-%20Issue%202.zip (accessed: Feb. 12 2021).

[17] K. Wackwitz and H. Boedecker, *Safety-Risk-Assessment-for-UAV-Operation: Safety Hazard Identification, Safety Risk SAFETY RISK ASSESSMENT FOR UAV OPERATION: Assessment, Safety Risk*

Mitigation Safety Risk Documentation + Case Study. [Online]. Available: https://www.thedroneprofessor.com/wp-content/uploads/2017/12/Safety-Risk-Assessment-for-UAV-Operation.pdf (accessed: Feb. 22 2021).

[18] L. C. Barr *et al.*, "Preliminary Risk Assessment for Small Unmanned Aircraft Systems," in *17th AIAA Aviation Technology, Integration, and Operations Conference*, Denver, Colorado, 2017.

[19] R. Weibel, M. Edwards, and C. Fernandes, "Establishing a Risk-Based Separation Standard for Unmanned Aircraft Self Separation," in *11th AIAA Aviation Technology, Integration, and Operations (ATIO) Conference*, Reston, Virigina, 2011.

[20] A. McFadyen and T. Martin, "Understanding Vertical Collision Risk and Navigation Performance for Unmanned Aircraft," in *37th DASC - Digital Avionics Systems Conference*, London, UK, 2018.

[21] A. McFadyen, T. Martin, and T. Perez, "Low-level collision risk modelling for unmanned aircraft integration and management," in *2018 IEEE Aerospace Conference 2018*, Big Sky, Montana, 2018, pp. 1–10.

[22] X. Zhang, Y. Liu, Y. Zhang, X. Guan, D. Delahaye, and L. Tang, "Safety Assessment and Risk Estimation for Unmanned Aerial Vehicles Operating in National Airspace System," *Journal of Advanced Transportation*, vol. 2018, 2018, doi: 10.1155/2018/4731585.

[23] S. Forster, H. Fricke, B. Rabillier, B. Hickling, B. Favennec, and K. Zeghal, "Analysis of safety performances for parallel approach operations with performance based navigation," in *Thirteenth USA/Europe Air Traffic Management Research and Development Seminar (ATM2019)*, Vienna, Austria, 2019.

[24] European Aviation Safety Agency, *Certification Specifications (CSs).* [Online]. Available: https://www.easa.europa.eu/document-library/certification-specifications/reg/initial-airworthiness (accessed: Mar. 16 2021).

[25] European Aviation Safety Agency, *'Drone Collision' Task Force: Final Report.* [Online]. Available: https://www.easa.europa.eu/document-library/general-publications/drone-collision-task-force (accessed: Mar. 20 2021).

[26] International Civil Aviation Organisation, *Procedures for Air Navigation Services (PANS) - Aircraft Operations - Volume II Construction Of Visual & Instrument Flight Procedures (Doc 8168).* [Online]. Available: https://store.icao.int/ (accessed: Mar. 20 2021).

[27] DWD Climate Data Center (CDC), *Historische 10-minütige Stationsmessungen der Max/Min -Mittel und Windspitzen in Deutschland.* [Online]. Available: https://opendata.dwd.de/

[28] DWD Climate Data Center (CDC), *Historische 10-minütige Stationsmessungen der mittleren Windgeschwindigkeit und Windrichtung in Deutschland.* [Online]. Available: https://opendata.dwd.de/

[29] Bundesamt für Kartographie und Geodäsie, "Digitales Geländemodell Gitterweite 200 m: DGM200," 2015. [Online]. Available: https://sg.geodatenzentrum.de/web_public/gdz/dokumentation/deu/dgm200.pdf

[30] Official Journal of the European Union, *COMMISSION IMPLEMENTING REGULATION (EU) No 923/2012: Regulation (EU) No 923/2012*, 2012.

[31] Eurocontrol, *EUROCONTROL Aircraft Performance Database.* [Online]. Available: https://contentzone.eurocontrol.int/aircraftperformance

[32] Eurocontrol, *SKYbrary.* [Online]. Available: https://www.skybrary.aero/

[33] European Aviation Safety Agency, *The European Plan for Aviation Safety (EPAS 2020-2024).* [Online]. Available: https://www.easa.europa.eu/sites/default/files/dfu/EPAS_2020-2024.pdf (accessed: Mar. 22 2021).

[34] M. Vogel, C. Thiel, and H. Fricke, "Assessing the air traffic control safety impact of airline pilot induced latencies," in *ATACCS'12:Proceedings of the 2nd International Conference on Application and Theory of Automation in Command and Control Systems*, London, UK, 2012.

[35] M. Vogel, C. Thiel, and H. Fricke, "A quantitative Safety Assessment Tool based on Aircraft Actual Navigation Performance," in *4th International Conference on Research and Air Transportation (ICRAT)*, Budapest, Hungary, 2010.

[36] International Civil Aviation Organisation, *Procedures for Air Navigation Services (PANS) - Aerodromes (Doc 9981).* [Online]. Available: https://store.icao.int/ (accessed: Mar. 20 2021).

[37] M. Brandt, *Fast 12 Millionen Sendungen pro Zustelltag - Nearly 12 million deliveries per day*. [Online]. Available: https://de.statista.com/infografik/9992/in-deutschland-von-den-paket-und-kurierdiensten-befoerderten-sendungen/ (accessed: Mar. 28 2021).

[38] S. Keller, *Anteile an der Gesamtsendungsmenge im KEP-Endkundenmarkt in Deutschland nach Anbietern im Geschäftsjahr 2017/18 - Consumer Market in Germnay 2017/18.* [Online]. Available: https://de.statista.com/statistik/daten/studie/893551/umfrage/anteile-der-paketdienste-an-der-gesamtsendungsmenge-in-deutschland/ (accessed: Apr. 11 2021).

[39] S. Keller, *Anzahl der Paketlieferungen pro Person und Jahr in ausgewählten Ländern (Stand: 2019).* [Online]. Available: https://de.statista.com/statistik/daten/studie/1016709/umfrage/paketsendungen-pro-person-und-jahr-in-ausgewaehlten-laendern/ (accessed: Mar. 11 2021).

[40] Statistisches Landesamt des Freistaates Sachsen, *Bevölkerung des Freistaates Sachsen jeweils am Monatsende ausgewählter Berichtsmonate nach 2020.* [Online]. Available: https://www.statistik.sachsen.de/html/bevoelkerungsstand-einwohner.html (accessed: Apr. 11 2021).

[41] Bundesnetzagentur, *Jahresbericht 2019: Netze für die digitale Welt.* [Online]. Available: https://www.bundesnetzagentur.de/SharedDocs/Pressemitteilungen/DE/2020/20200429_Jahresbericht.html (accessed: Apr. 11 2021).

[42] E. Sunil, J. Ellerbroek, and J. Hoekstra, *Metropolis - Urban Airspace Design: Scenario Definition Report (D1.2).* [Online]. Available: http://homepage.tudelft.nl/7p97s/Metropolis/downloads/Metropolis_D1_2_Scenario%20Definition%20Report-v0_08.pdf (accessed: Apr. 11 2021).

[43] J. Hoekstra, S. Kern, O. Schneider, F. Knabe, and B. Lamiscarre, *Metropolis - Urban Airspace Design: Societal Demand & Technology Review (D1.1).* [Online]. Available: http://homepage.tudelft.nl/7p97s/Metropolis/downloads/Metropolis_D1_1_Report%20on%20Societal%20Demand%20%20Technology%20review-v1_0.pdf (accessed: Apr. 10 2021).

AUTHOR BIOGRAPHY

Hartmut Fricke studied and got his PhD in Aeronautics and Astronautics at Technische Universität (TU) Berlin, was then a research fellow in Flight Operations, Airport Planning, and ATM at TU Berlin. In 2001 he received the grade Habilitation on "Integrated Collision Risk Modeling for airborne and ground-based systems". Since then, he has been Head of the Institute of Logistics and Aviation, at Technische Universität (TU) Dresden.

William J. Austen studied Mechanical Engineering at the University of Durham, UK before joining DERA/QinetiQ in 2001 as a structural analyst. William is now responsible for the Structural Analysis and Optimization capability at QinetiQ, Farnborough where he leads advanced simulation projects across aerospace, maritime, weapons, space and land domains. William is a Fellow of the Institution of Mechanical Engineers and a QinetiQ Fellow. Current activities include technical leadership of the Horizon 2020 Vulnerability of Manned Aircraft to Drone Strikes programme for EASA.

Stanley Förster studied Computer Science at Technische Universität (TU) Dresden. Since October 2015, he is a research fellow at the Chair of Air Transport Technology and Logistics.

Christoph Thiel studied Aeronautics and Astronautics at Technische Universität (TU) Berlin. In August 2002 he became an employee at Gesellschaft für Luftverkehrsforschung mbH (GfL). From 2009 to 2015 he was a research fellow in Flight Safety and ATM at Technische Universität (TU) Dresden (Chair of Air Transport Technology and Logistics). Since then, he is senior consultant at GfL.

Robert Brühl studied Transport Engineering at Technische Universität (TU) Dresden. Since November 2017, he is a research fellow at the Chair of Air Transport Technology and Logistics.